Metal/Ceramic Thin Film Adhesion Measured by Cross-Sectional Nanoindentation

M.R. Elizalde[1], J.M. Sánchez[1], J.M. Martínez-Esnaola[1], D. Pantuso[2], T. Scherban[2], B. Sun[3] and J. Xu[2]

[1] CEIT (Centro de Estudios e Investigaciones Técnicas de Gipuzkoa) and Escuela Superior de Ingenieros, TECNUN (Universidad de Navarra), Paseo de M. Lardizábal 15, 20018 San Sebastián, Spain.
[2] Intel Corp., 2501 NW 229th Avenue, Hillsboro, Oregon 97124, USA.
[3] Intel Corp., 3065 Bowers Avenue, Santa Clara, California 95051, USA.

ABSTRACT: *Thin film interfacial adhesion is a critical property in assessing thermo-mechanical reliability of microelectronic components. This work presents a novel technique, the cross-sectional nanoindentation (CSN), which has been applied to the study of metal/ceramic thin film stacks deposited on a Si substrate. During a CSN test, a nanoindentation is made in the cross-section of the Si substrate at a distance from the interface that produces controlled bending of the outer thin film and the formation of a crack at the interface of interest. The test is modelled by FEM to calculate the interfacial energy. The results obtained are in good agreement with the values measured using four point bending (4 PB), which is the standard procedure used to date in the microelectronics industry. The advantages of the CSN test are that it is quick, sample preparation is extremely easy and the crack path can be observed by SEM. Unlike 4 PB, CSN gives a local measurement of adhesion, producing delaminations of similar size to those found in integrated circuit failures. This higher spatial resolution suggests a natural extension of the technique to the study of delamination in patterned structures.*

INTRODUCTION

Understanding of thin film (TF) interfacial cracking is a critical reliability concern, as this fracture phenomenon has been identified in the origin of many short-circuit failures, not only in integrated circuits (IC) production but also during device operation [1]. Therefore, a technique to measure the intrinsic interfacial strength is needed. Among the developed techniques [2,3], the four point bending test (4 PB) is a widely accepted method within the IC industry for measuring interfacial toughness in thin film multilayer structures [4]. However, the bending technique is only applicable to blanket (i.e., not patterned) materials, is time consuming and requires surface chemical analysis to determine which interface debonded.

The cross sectional nanoindentation (CSN) test, first introduced by our group in 1999 [2], is a quick technique, applicable to patterned structures, that allows direct observation of the delamination crack tip. It has been successfully applied to Si_xN_y-SiO_2 thin film stacks (where the thin film behaviour is purely elastic). This paper represents an extension of our previous work to metal-ceramic interfaces.

EXPERIMENTAL PROCEDURE

Sample preparation

The thin film stacks consisted on electroplated Cu/barrier (250 Å)/SiO_2 deposited on silicon wafers using the Damascene process [5]. Samples were prepared with two Cu barrier types, X (samples *A*, *C*, *E*) and Y (*B*, *D*, *F*), and three Cu film thicknesses, 0.26 µm (samples E, F), 0.5 µm (samples C, D) and 1.0 µm (samples A, B.) (Table 1). Barrier X is known to give better adhesion than barrier Y.

Cross sections were prepared by cleavage of the wafers by scratching on the Cu film with a diamond tip and subsequent bending with special glasscutter's pliers. The cross sections obtained are flat and clean, and no further polishing is required. Samples obtained from the same wafers were prepared to carry out four-point bending tests [6].

CSN test description

CSN tests [2] were carried out with a Nano Indenter II© (Nano Instruments, USA) in load control at 500 µN/s and spaced 200 µm apart. The distance from the indentation to the Cu-SiO_2 interface (*d*) was selected depending on the Cu thickness in order to avoid tearing of the Cu film during crack propagation. A distance between 4 and 5 µm was used for samples with thicknesses of 0.5 and 1.0 µm. For the 0.26 µm Cu film, this distance was reduced to 3 – 4 µm. After maintaining the maximum load (between 70 mN and 120 mN) for 5 seconds, the load was released at the same rate used for loading. The samples were subsequently analised by scanning electron microscopy (SEM).

CSN RESULTS

A typical interfacial crack produced by CSN is shown in Fig. 1. For each test, the interfacial crack length (*x*), the wedge length (2*b*), the wedge

displacement after load removal (u_f) and the distance from the indent to the interface of interest (d) are measured from SEM micrographs.

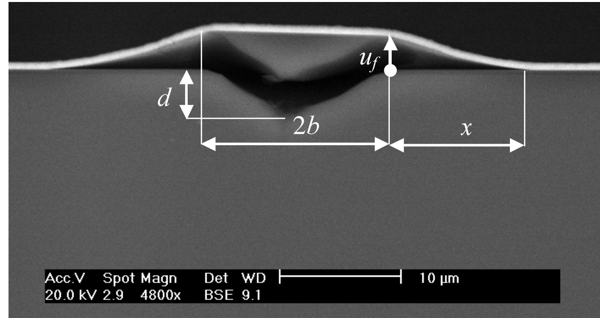

Figure 1: SEM micrograph of a CSN test performed on sample *A*.

As obtained by 4PB [4], CSN tests have shown that, for the Cu-barrier-SiO_2 system, debonding occurs at the barrier-SiO_2 interface, since the barrier film appears stuck to the Cu film after testing (Fig. 2a) and shows parallel small cracks. However, for sample *A* (1 µm Cu, barrier X), 93 % of the tests show ligaments adhered to the Cu film whereas pieces of barrier appear on the SiO_2 (Fig. 2b). In this case, the interfacial crack seems to progress alternatively through the Cu-barrier and the barrier-SiO_2 interfaces.

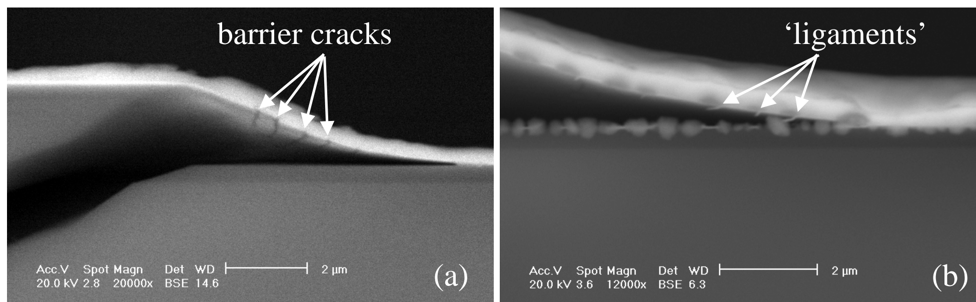

Figure 2: SEM micrographs of CSN tests on samples (a) *F* and (b) *A*.

Finally, Figures 3 and 4 show the debonded area calculated from the measured wedge and crack lengths (assuming a semi-circular delaminated area [2]) versus the wedge displacement after load removal for the different Cu TF thicknesses. These results show a high dispersion, especially in the case of samples with barrier Y (having worse interfacial adhesion). However, the barrier X samples (*A*, *C*, *E*), with better adhesion, show a lower debonded area for the same wedge displacement. The large dispersion found in delaminated areas suggests that interfacial adhesion is not

homogenous but subjected to local changes (contrary to that assumed in 4 PB).

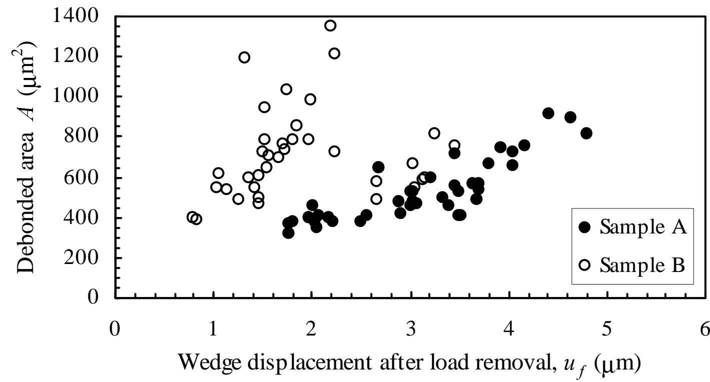

Figure 3: Debonded area A vs. wedge displacement after load removal, u_f, for samples with 1 µm Cu TF thickness.

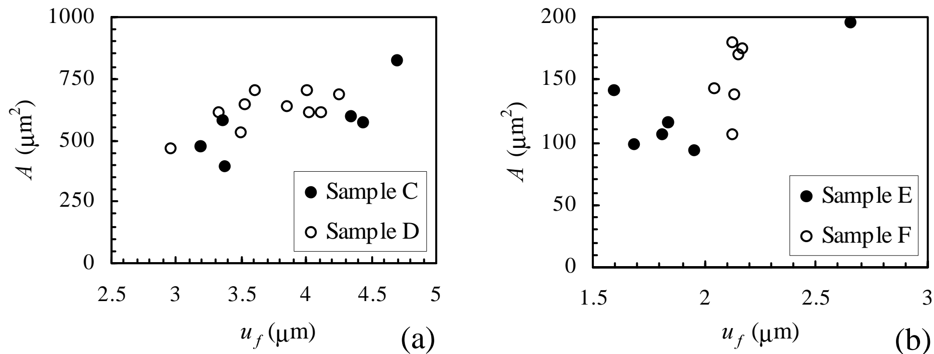

Figure 4: Debonded area A vs. wedge displacement after load removal, u_f, for samples with (a) 0.5 µm Cu and (b) 0.26 µm Cu TF thickness.

MODELLING

Model description

Unlike ceramic-ceramic systems [2], CSN test on a metal-ceramic system is modelled using finite elements (ABAQUS) as an axisymmetric (circular) plate (axisymmetric 8-node quadrilateral elements) with the nodes at the bonded portion of the Cu-SiO_2 clamped and a vertical displacement

imposed to the nodes in contact with the wedge (Fig. 5). The maximum wedge displacement u_0 is chosen such that the wedge displacement after removing the load at the end of the FEM simulation matches the one measured in the SEM on the corresponding CSN test, u_f. The outer Cu TF is considered as elastic, perfectly plastic.

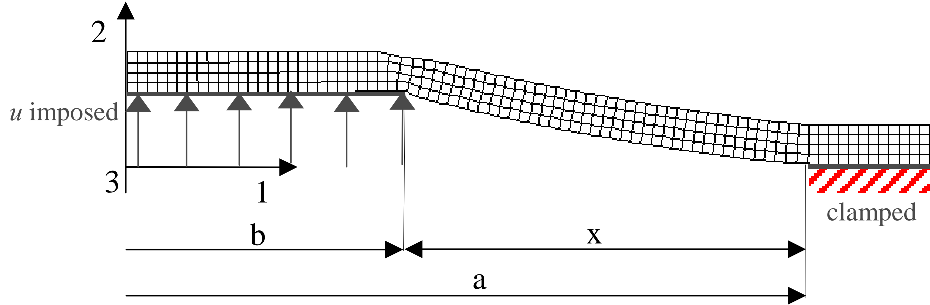

Figure 5: Sketch of the CSN FEM model.

The model inputs are the thickness of the Cu TF, h, the parameters measured by SEM after each CSN test (b, x and u_f, Fig. 1) and the elastic modulus, E, Poisson ratio, ν, and yield stress σ_y of the Cu TF. In the simulations the values E = 165 GPa, $\nu = 0.28$ and a $\sigma_y = 524 \pm 18$ MPa for sample A and $\sigma_y = 544 \pm 8$ MPa for sample B have been used. The elastic modulus has been measured with a NanoIndenter XP^{TM} (MTS, USA) [7], using a sharp Berkovich tip and a continuous stiffness modulation unit, and the yield strength for the 1 μm thick Cu TF with a Hysitron Triboscope [8]. For thinner films (0.5 and 0.26 μm), this method is not applicable, since TF surface roughness is too high compared to the piling up created by the indentation. For these specimens, the data obtained for sample B is used.

For this analysis, crack propagation has been simulated in 20 steps. This means that the crack is divided in 20 intervals. At the beginning of the simulation only the first interval of the crack is debonded. For simplicity, a linear relationship has been assumed between crack growth and wedge displacement during a CSN test. Two cases are considered depending on the sequence in which the displacement is imposed and the crack is debonded. In the case without relaxation, in each step 1/20 of the nodes of the interfacial crack are debonded and simultaneously the wedge displacement is incremented in 1/20 of the total u_0. In the case with relaxation, each incremental wedge displacement and crack debonding is simulated in two steps: in a first step the wedge displacement is incremented in 1/20 of the total displacement u_0 and in the next step 1/20 of the interfacial crack nodes are debonded.

Calculation of interfacial debonding energy
Two values of the interfacial debonding energy are calculated, one from the simulation with relaxation, which corresponds to the definition of the elastic energy release rate G, and another from the simulation without relaxation.

In the case without relaxation, the interfacial energy T_i is calculated considering that the total strain energy U stored in the Cu film is spent in crack surface formation. Obviously, part of the energy will be spent in deforming the Cu film and not in creating the interfacial crack. But as in 4 PB tests the plastic strain energy consumed by the film is attributed to the interface, the total strain energy is the value to consider if we want to compare the results of both techniques. This is computed numerically as:

$$T_i = \frac{\Delta U}{\Delta A} \quad (1)$$

According to the above convention, the energy consumption is calculated from the slope of the U vs. debonded area curve. The mode mixity has been calculated from the stresses at nodes corresponding to the crack tip obtained in the FEM simulations. A value of about 45-50º has been obtained, which is comparable to the value of 43º calculated for the 4 PB test [4,6].

In the case with relaxation, an elastic strain energy U_e release is observed (Fig. 6) for the steps where the wedge displacement is maintained while the crack grows. This energy is spent in crack area formation, $G_c \Delta A$, and additionally, a certain amount of energy may be used to further deform plastically the Cu film (the simulations indicate that the plastic strain energy U_p slightly increases during the relaxation step). A debonding energy release rate, G_c, can be calculated, according to the energy balance:

$$\Delta U_e + \Delta U_p + G_c \Delta A = 0 \quad (2)$$

The values of the interfacial debonding energy calculated from FEM CSN test simulations with and without relaxation and from 4 PB tests are gathered in Table 1. It is noticeable that the values obtained from CSN tests using the total strain energy compare very well with the values given by the 4 PB tests. For each Cu thickness, a difference in T_i is observed between samples with barrier X and barrier Y. The effect of attributing the plastic energy consumed by the Cu TF to the interface is reflected in the dependence of T_i on the Cu TF thickness: the interfacial energy is higher for thicker Cu TF. It should be noted that the dispersion in the results is higher

for CSN than for 4 PB. As previously stated, this result reflects the fact that CSN is a local test that produces delaminated areas of about 500-1000 μm^2 whereas 4 PB test produces delaminated areas of 10^7-10^8 μm^2.

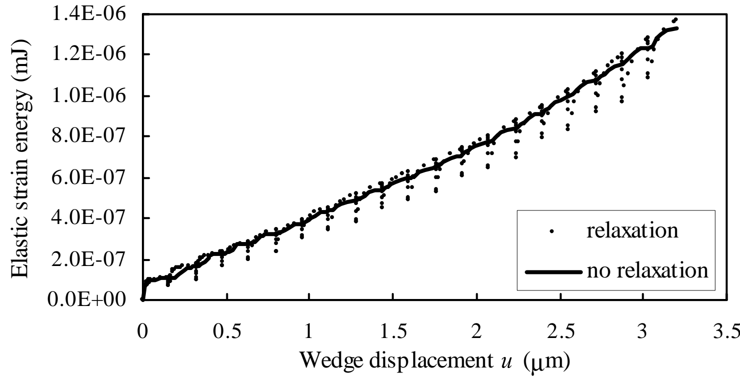

Figure 6: Elastic strain energy vs. wedge displacement curve of a CSN test FEM simulation performed with and without relaxation (Sample *A*).

Table 1: Interfacial debonding energy as calculated from CSN tests (with G_c and without relaxation T_i) and from 4 point bend tests T_i. Mean values and 95% C.I.

Sample	T_i (CSN, J.m^{-2})	T_i (4PB, J.m^{-2})	G_c (J.m^{-2})
A (1 μm, barrier X)	24.1 ± 2.1 (19 tests)	16.1 ± 0.8	1.44
B (1 μm, barrier Y)	14.6 ± 2.3 (6 tests)	12.1 ± 0.8	1.34
C (0.5 μm, barrier X)	13.5 ± 3.9 (5 tests)	13.2 ± 1.1	1.01
D (0.5 μm, barrier Y)	9.8 ± 1.2 (10 tests)	10.8 ± 1.3	0.94
E (0.26 μm, barrier X)	13.2 ± 5 (6 tests)	11.9 ± 0.7	-
F (0.26 μm, barrier Y)	10.8 ± 3.4 (6 tests)	10.2 ± 0.8	-

Finally, the values obtained from FEM simulations with relaxation are one order of magnitude lower than those obtained from the total strain energy. These data, ranging from 0.94 to 1.44 J/m^2, are similar to those predicted by the dislocation free zone model (DFZ) [9] and could be closer to the intrinsic interfacial energy.

CONCLUSIONS

The cross-sectional nanoindentation technique has been demonstrated to be a reliable test method applicable to metal-ceramic thin film stacks with thicknesses ranging from 0.26 to 1 μm. The results obtained clearly show that the technique can resolve differences in adhesion strength. Its advantages are ease of sample preparation, quick turn-around time and direct observation of the delamination crack path. For metal-ceramic

systems FEM is necessary to calculate the plastic contribution of the metal thin film. The results obtained show good correlation to four point bending results when the plastic work consumed by the thin film is attributed to the interface. When this effect is separated, an intrinsic value of the interfacial energy is obtained. Finally, delamination areas obtained by CSN are close in size to those found in IC failures. This higher spatial resolution suggests a natural extension of the technique to the study of delamination in patterned structures. In fact, in a preliminary study, CSN showed the ability of distinguishing differences in delamination behaviour due to local geometry effects [10].

ACKNOWLEDGEMENTS

The authors gratefully acknowledge the financial support of Intel Corporation for the realisation of this work. M.R.E. and J.M.M.E. are grateful to the 'Ministerio de Educación y Cultura' (Spanish Government) and to the Basque Government for the funds received. Jeanette Blaine of Intel is acknowledged for providing the yield strength measurements.

REFERENCES

1. Lane, M., Vainchtein, A., Gao, H. (2000) *J. Mater. Res.* **15**, 2758.
2. Sánchez, J.M., El-Mansy, S., Sun, B., Scherban, T., Fang, N., Pantuso, D., Ford, W., Elizalde, M.R., Martínez-Esnaola, J.M., Martín-Meizoso, A., Gil-Sevillano, J., Fuentes, M., Maiz, J. (1999) *Acta Mater* **47**, 4405.
3. Martínez-Esnaola, J.M., Sánchez, J.M., Elizalde, M.R., Martín-Meizoso, A. (2000), In: *Fracture Mechanics: Applications and Challenges*, pp. 47-71, Fuentes, M., Elices, M., Martín-Meizoso, A., Martinez-Esnaola, J.M. (Eds). Elsevier, Amsterdam.
4. Lane, M., Dauskardt, R.H., Krishna, N., Hashim, I. (2000) *J. Mater. Res.* **15**, 203.
5. Maydan, D. (2001) *Mat. Sci. & Eng.* **A302**, 1.
6. Ma, Q. (1997) *J. Mater. Res.* **12**, 840.
7. Oliver, W.C., Pharr, G.M. (1992) *J. Mater. Res.* **7**, 1564.
8. Kramer, D., Huang, H., Kriese, M., Robach, J., Nelson, J., Wright, A., Bahr, D., Gerberich, W.W. (1999) *Acta. Mater.* **47**, 333.
9. Volinsky, A.A., Moody, N.R., Gerberich, W.W. (2002) *Acta Mater* **50**, 441.
10. Sun, B., Scherban, T., Pantuso, D., Sánchez, J.M., Elizalde, M.R., Martinez-Esnaola, J.M. (2001) *10th ICF Proc.*, 2-6 Dec. 2001, Hawaii.